New Ferrocene Based Thiourea and Guanidines: Synthesis, Structural Elucidation, Aggregation Properties, DNA Binding Studies, and DFT calculations

Maria Azeem, Jahangeer Ali Patujo, Saira Fatima, Amin Badshah*, Laiba Saleem and Saif-ur-Rehman
Coordination Chemistry Laboratory, Department of Chemistry,
Quaid-i-Azam University (45320) Islamabad, Pakistan.
aminbadshah@yahoo.com*

Summary: One new ferrocenyl thiourea and four new ferrocene-based alkyl guanidines have been successfully synthesized and well characterized by FT-IR, ^{1}H and ^{13}C NMR. Aggregation properties of ferrocene-based guanidines have been assessed by determining their critical micelles concentration through tensiometry and UV-Visible spectroscopy in the ethanol solution. The results obtained through both the techniques were in close agreement. DFT calculations were performed to calculate the charges distribution, E_{HOMO}, E_{LUMO} and band gaps of synthesized compounds which were further supported through UV-Visible spectroscopy. Due to the ability of ferrocene and guanidine compounds to bind with DNA, their DNA binding studies were performed through cyclic voltammetry and UV-Visible spectroscopy. Binding constant values of the guanidine derivatives are higher than the thiourea and have a linear dependence on the lipophilicity.

Keywords: Ferrocene, Guanidines, Surfactants, Critical micelles concentration, Micelles, Density functional theory.

Introduction

In last few decades, guanidine derivatives have been acquired a significant importance due to their biological and synthetic importance, thermodynamic stability and high basic strength [1]. A guanidine molecule has very high bronsted basicity that is very close to OH [2]. The substitution of electron withdrawing or electron donating groups can adjust its basicity and lipophilicity.

The guanidine or guanidinium ion also exist in the pyrimidine bases of DNA, the muscular energy-intermediate creatine, the amino acid arginine, and a number of other biologically active molecules [3]. The strong basic structure of guanidine is responsible for constraining the DNA synthesis and blocking the Na$^+$ movement across the nerve membrane that hinders the nerve functioning. These properties gave an idea to use them in anticancer drugs [4]. (2-(2, 5-dimethoxyphenylthio)-6-methoxybenzylideneamino) guanidine, Spergualin and a series of 1-[2-alkylthio-5-(azol-2 or 5-yl)-4-chlorobenzenesulfonyl]-3-hydroxyguanidines are considered to possess anticancer activity [5-7].

Incorporation of ferrocene to an organic structure enhances its biological activity because of owing lipophilic character, ð-conjugated system, redox activity and low cytotoxicity against the living systems and high cytotoxicity against the tumor ability [8]. Lal *et al.* observed that ferrocene substituted thioureas have substantial action against cancerous cells. Ferrocene in comparison to other metal scaffolds is considered itself as non-toxic (half-life of ferrocene in rats is 200 days for bronchopulmonary region) but it depend on its functionalization. Acetylferrocene is most toxic derivative whose lethal dose is 5-50 mg/kg for the male rats [9] On the other hand, a number of ferrocenyl derivatives have good medicinal activities. Ferrocene can also improve the antimalarial activity of quinine, mefloquine and chloroquine by enhancing their role in the processes that involve the generation and quenching of free radicals. Due to the ease of oxidation of Fc^{+2}, it plays an active role in the redox cycling which may contributes to the antiplasmodial activity [10-11]. An anti-cancer drug ferrocifin is formed by the replacement of aromatic ring of tamoxifen (anti-cancer drug) with ferrocenyl group and has showed higher activity against breast cancer cells [12]. Due to electronic properties and easy functionalization of ferrocene, it has many applications in the material chemistry as aerospace materials, sensors, catalysts and electroactive materials [13-15]. Zhang and co-workers synthesized ferrocene based cross-linked micelle system by using cross linking agent 1, 1′- ferrocene dicarboxylic acid. This study showed that ferrocene containing micelle system has a significant cytotoxicity against the HeLa cells [16]. Self-aggregating properties of bipolar molecules in the mixture of organic/aqueous have found applications in the template syntheses of inorganic materials and micelles help to control the pore size of nonporous materials [14-16]. Ethanol is most commonly used as additive in this template

---

*To whom all correspondence should be addressed.

synthesis due to the lower solubility of many organic reactants in pure aqueous media [17-19].

Keeping in view, the biological and aggregation relevance of ferrocene and guanidine, the synthesis of ferrocene appended guanidines has been undertaken. Their aggregation behavior is determined through the critical micelles concentrations assessment. In order to initially probe their anticancer potency it was decided to explore their DNA binding properties. Computational study was also conducted to evaluate the energies of molecular orbitals and charge densities of different atoms of synthesized compounds.

Experimental

Chemicals and Instrumentation

The chemicals *i.e* heptylamine, dodecylamine, hexadecylamine, octadecylamine, benzoyl chloride, ferrocene, 2-methyl-4-nitoaniline, sodium nitrite, potassium thiocyanate, hydrochloric acid, hydrazine and mercuric chloride were obtained from Sigma-Aldrich, Fluka and E. Merck. All the solvents including diethyl ether, ethanol, petroleum ether, acetone, n-hexane, dimethyl formamide, chloroform, and methanol were dried and distilled through the standard drying methods. Infrared spectra (FT-IR) for the synthesized compounds were recorded through Thermo Scientific Nicolet-6700 FTIR spectrometer having frequency range from 400-4000 cm^{-1}. The instrument used to record the ^{1}H and ^{13}C spectra of the synthesized compounds was 300 MHz BRUKER AVANCE NMR spectrometer having trimethylsilane (*TMS*) as an internal reference.

General Synthesis Procedure

The synthesis procedure comprises three main steps. A complete sketch of the synthetic procedure is given in the Scheme-1. First step includes the synthesis of nitro phenyl ferrocene and its reduction into ferrocenyl aniline according to the methods reported by our research group [20-21]. In the second step, benzoyl isothiocyanate was synthesized by adding the benzoyl chloride to the potassium thiocyanate in anhydrous acetone, heated for 10 to 20 minutes and stirred for 2 h. The resulting product was treated with ferrocenyl aniline and stirred for 24 h to obtain the desired ferrocenyl thiourea [19]. This product was poured into ice cooled water, stirred for 1 h, filtered, washed with distill water, dried and recrystallized through acetone. In the third step, ferrocene based guanidine surfactants were synthesized by treating the ferrocenyl thiourea with different long chain amines in dimethyl formamide (DMF). To the reaction mixture, two equivalents of trimethylamine were added below 5 ^{o}C. One equivalent

of mercuric chloride was also added to the reaction mixture for the removal of sulfur. Temperature below 5 ^{o}C was maintained for 4 to 5 h. Reaction progress was monitored through TLC. After the overnight stirring, 15 to 25 mL of chloroform was added to reaction mixture and filtered to remove HgS. DMF was removed through the solvent extraction method and other solvents were evaporated [22-24]. (Scheme-1).

*1-(benzoyl) -3-(4-ferrocenyl, 3-methylphenyl) thiourea (**FTU**)*

FT-IR (ATR cm^{-1}): 483 (Fe-Cp), 1245 (C=S), 1681 (C=O), 3032 (Ar-H), 3100 (NH); ^{1}H NMR (300 MHz, DMSO-d$_6$, δ-ppm): 12.67 (s, 1H, ^{1}NH), 11.58 (s, 1H, ^{2}NH), 7.60-8.01 (m, 9H, Ar-H), 4.825 (s, 2H, C$_5$H$_4$), 4.247 (s, 2H, C$_5$H$_4$), 4.054 (s, 5H, C$_5$H$_5$),; ^{13}C NMR: (75 MHz, DMSO-d$_6$, δ-ppm): 178.9 (C=S), 168.7 (C=O), 137.6, 136.1, 133.6, 132.6, 129.1, 128.9, 126.3, 124.3, (Ar-C), 84.6 (*ipso* C, C$_5$H$_4$), 69.8 (2C, C$_5$H$_4$), 69.4 (2C, C$_5$H$_4$), 66.7 (5C, C$_5$H$_5$).

*N-(4-Ferrocenyl,　　　　　phenyl)-N$'$-(octadecyl)-N$''$-benzoylguanidine (**R-18G**)*

FT-IR (ATR cm^{-1}): 482 (Fe-Cp), 1699 (C=O), 2960-2849 (sp^3 CH), 3086 (Ar-CH$_2$), 3129 (NH), 3223 (NH); ^{1}H NMR (300 MHz, DMSO-*d^6*, δ-ppm): 11.03 (s, 1H, ^{1}NH), 10.82 (s, 1H, ^{2}NH), 7.38-8.05 (m, 9H, Ar-H), 4.33 (s, 2H, C$_5$H$_4$), 4.76 (s, 2H, C$_5$H$_4$), 4.028 (s, 5H, C$_5$H$_5$), 2.54 (s, 2H, ^{1} CH$_2$), 1.62 (s, 2H, ^{2}CH$_2$), 1.60 (s, 2H, ^{3}CH$_2$), 0.85-1.50 (m, 28H, $^{4-17}$CH$_2$), 0.83 (m, 3H, ^{18}CH$_3$); ^{13}C NMR: (75 MHz, DMSO-*d^6*, δ- ppm): 169.1 (C=O), 151.4 (CN$_3$), 135.9, 134.8, 133.5, 132.7, 129.0, 128.7, 128.6, 128.0, 127.9, 126.7, 126.3, 120.3 (12C, Ar-C), 85.1(*ipso* C, C$_5$H$_4$), 69.8 (2C, C$_4$H$_5$), 66.6 (2C, C$_5$H$_4$), 66.4 (5C, C$_5$H$_5$), 29.4 (1C, ^{1}C), 29.1 (15C, $^{2-16}$C), 22.5 (1C, ^{17}C), 14.4 (1C, ^{18}C).

*N-(4-Ferrocenyl,　　　　　phenyl)-N$'$-(hexadecyl)-N$''$-benzoylguanidine (**R-16G**)*

FT-IR (ATR cm^{-1}): 482 (Fe-Cp), 1683 (C=O), 2959-2850 (sp^3 CH), 3070 (Ar-CH$_2$), 3125 (NH), 3225 (NH); ^{1}H NMR (300 MHz, DMSO-*d^6*, δ-ppm): 11.03 (s, 1H, ^{1}NH), 10.6 (s, 1H, ^{2}NH), 7.3-8.01 (m, 9H, Ar-H), 4.83 (s, 2H, C$_5$H$_4$), 4.76 (s, 2H, C$_5$H$_4$), 4.01 (s, 5H, C$_5$H$_5$), 1.60 (2H, ^{1}CH$_2$), 1.58 (t, 2H, ^{2}CH$_2$), 0.85-1.50 (m, 26H, $^{3-15}$CH$_2$), 0.82 (t, 3H, ^{16}CH$_3$); ^{13}C NMR: (75 MHz, DMSO-d$_6$, δ- ppm): 169.7 (C=O), 151.2 (CN$_3$), 135.1, 134.6, 133.6, 132.7, 129.3, 128.7, 128.6, 128.0, 127.4, 126.7, 126.3, 120.7 (12C, Ar-C), 85.4 (*ipso* C, C$_5$H$_4$), 69.5 (2C, C$_5$H$_4$), 66.6 (2C, C$_5$H$_4$), 66.4 (5C, C$_5$H$_5$), 30.4 (1C, ^{1}C), 29.1 (13C, $^{2-14}$C), 22.3 (1C, ^{15}C), 13.7 (1C, ^{16}C)
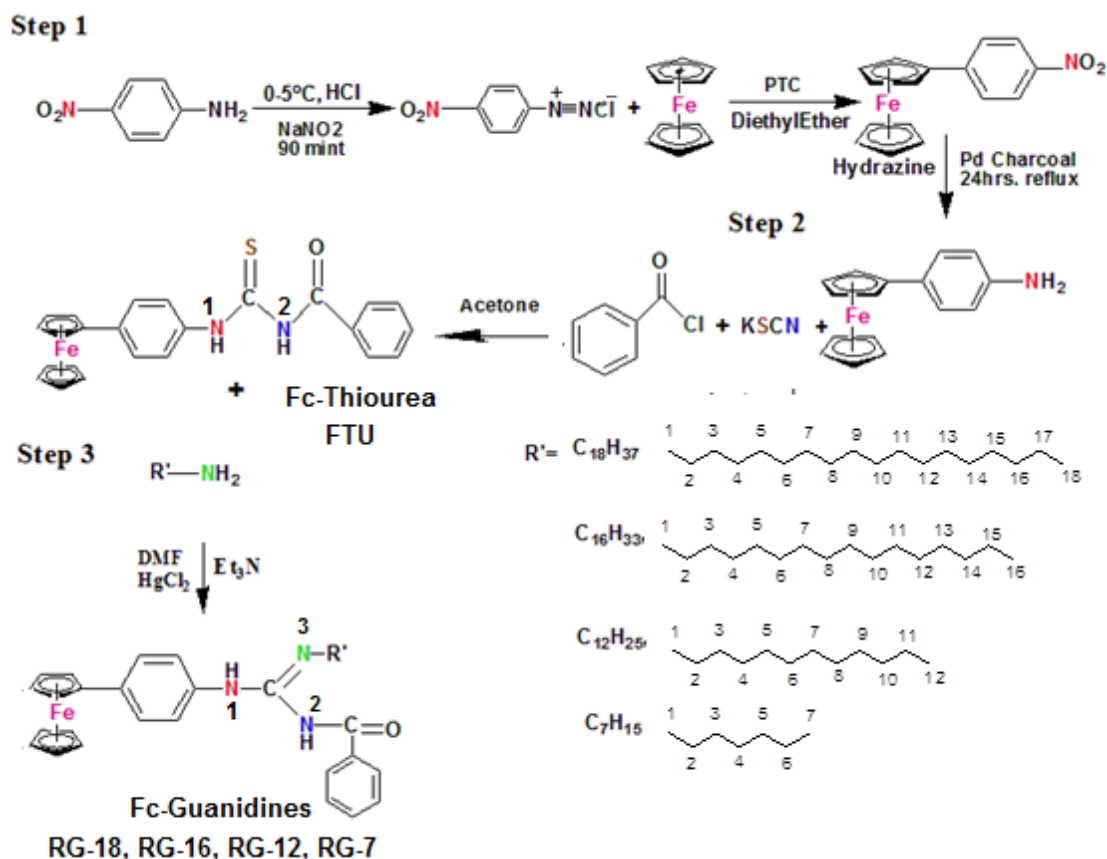
Scheme-1: Synthesis pathway of ferrocenyl thiourea and guanidine derivatives.

N-(4-Ferrocenyl, phenyl)-N′-(dodecyl)-N″-benzoylguanidine (R-12G)

FT-IR (ATR cm^{-1}): 482 (Fe-Cp), 1698 (C=O), 2955-2850 (sp^3 CH), 3054 (Ar-CH$_2$), 3115 (NH), 3229 (NH); ^{1}H NMR (300 MHz, DMSO-d^6, δ-ppm): 10.9 (s, 1H, ^{1}NH), 9.92 (s, 1H, ^{2}NH), 7.43-8.25 (m, 9H, Ar-H), 4.31 (s, 2H, C$_5$H$_4$), 4.74 (s, 2H, C$_5$H$_4$), 4.05 (s, 5H, C$_5$H$_5$), 2.07-1.29 (m, 22H, $^{1-11}$CH$_2$), 0.88 (t, 3H, ^{12}CH$_3$); ^{13}C NMR: (75 MHz, DMSO-d_6, δ- ppm): 169.3 (C=O), 151.1 (CN$_3$), 135.3, 134.4, 133.5, 132.3, 129.2, 128.7, 128.6, 128.0, 127.7, 126.7, 126.3, 120.4 (12C, Ar-C), 85.0 (*ipso* C, C$_5$H$_4$), 69.5 (2C, C$_5$H$_4$), 66.6 (2C, C$_5$H$_4$), 66.4 (5C, C$_5$H$_5$), 32.3 (1C, ^{1}C), 29.5 (9C, $^{2-10}$C), 22.3 (1C, ^{11}C), 14.1 (1C, ^{12}C).

N-(4-Ferrocenyl, phenyl)-N′-(heptyl)-N″-benzoylguanidine (R-7G)

FT-IR (ATR cm^{-1}): 483 (Fe-Cp), 1700 (C=O), 2952-2853 (sp^3 CH), 3032 (Ar-CH$_2$), 3085 (NH), 3232 (NH) ; ^{1}H-NMR (300 MHz, DMSO-d^6, δ-ppm): 10.84 (s, 1H, ^{1}NH), 10.25 (s, 1H, ^{2}NH),

7.45-8.04 (m, 9H, Ar-H), 4.34 (s, 2H, C$_5$H$_4$), 4.78 (s, 2H, C$_5$H$_4$), 4.03 (s, 5H, C$_5$H$_5$), , 2.9-1.2 (m, 12H, $^{1-6}$CH$_2$), 0.86 (s, 3H, ^{7}CH$_2$); ^{13}C NMR: (75 MHz, DMSO-d_6, δ- ppm): 169.5 (C=O), 151.3 (CN$_3$), 135.5, 134.2,133.6, 132.3, 129.5, 128.7, 128.6, 128.0, 127.6, 126.7, 126.3, 120.1 (12C, Ar-C), 85.0 (*ipso* C, C$_5$H$_4$), 69.8 (2C, C$_5$H$_4$), 66.6 (2C, C$_5$H$_4$), 66.4 (5C, C$_5$H$_5$), 28.7 (4C, $^{1-4}$C), 22.4 (2C, $^{5-6}$C), 14.3 (1C, ^{7}C).

Interfacial and Aggregation Properties of Ferrocene Based Guanidine Surfactants

Surfactants at low concentration have a property to adsorb at the surface or interfaces of system (solid-solid, liquid-solid, and liquid-liquid). This unique property of surfactants can be studied through different methods for example conductometry, UV-Visible spectroscopy, scattering, fluorescence spectroscopy, surface tension measurements *etc*. In this study the methods used for the assessment of critical micelle concentration of synthesized ferrocenyl guanidine surfactants are surface tension and UV- Visible spectroscopy.

Determination of CMC through UV-Visible Spectroscopy

A spectrum was obtained through the UV-Visible method to determine the critical micelles concentration of synthesized ferrocene based guanidine surfactant. Solutions of different concentrations (0.0005-2 mM) were prepared in ethanol as all the synthesized guanidine surfactants are completely soluble in the ethanol. Equal volume of solvent (3 mL) was taken in both the reference and working cell to avoid the intervention of solvent. A graph of absorbance *vs.* concentration in mM was plotted and an inflection point was labelled as critical micelles concentration (CMC) [25].

Determination of CMC through Surface Tension Measurements

Automatic surface tensiometer was used for determining the CMC of synthesized surfactants. De Nouy ring method was followed for this purpose. A platinum ring was washed and dried completely and an instrument was calibrated before taking the readings. The surface tension of ethanol was measured as 22 mN/m at 25 ^{o}C. Solutions of different concentrations between 0.0003-2 mM were prepared. By the addition of surfactant to ethanol, surface tension decreases which can be observed through the readings appeared on screen. *CMC* was determined by plotting a graph between the surface tension and concentration (Fig. 2).

Computational Studies

Due to the simplicity and less time consumption, density functional theory (DFT) method was used to determine [19] *HOMO, LUMO* orbitals and mulliken's charge densities of synthesized compounds using the 6-31G base set. All the computational calculations were carried out in p-4 and the software used was GAUSSIAN 03 W.

DNA Binding Studies

UV-Visible Spectroscopy

The stock solutions of ferrocenyl guanidine surfactants were prepared in the ethanol. Commercial salmon sperm DNA (SS-DNA) obtained from Sigma Aldrich (Cat. No. 74782) was solubilized in in the deionized water. Concentration of DNA was find out through the molar extinction coefficient $\varepsilon = 6600$ M^{-1} cm^{-1} at 260 nm. The ratio of absorbance at 260 nm and 280 nm was calculated to check the purity of DNA. The ratios of absorbance at 260 nm/absorbance

at 280 nm were in range of 1.80-1.90, which indicate that the DNA is free from the protein. Firstly, absorbance of compounds was measured without the DNA addition. By keeping the compound concentration constant and adding different concentrations of DNA at regular intervals of time, UV-Visible spectra were obtained. Binding constants for all compounds were calculated by using the equation 1 [26].

$$\frac{Ao}{A - Ao} = \frac{\varepsilon G}{\varepsilon H - G - \varepsilon G} + \frac{\varepsilon G}{\varepsilon H - G - \varepsilon G} \frac{1}{K[DNA]} \quad (1)$$

Cyclic Voltammetry

For cyclic voltammetry stock solutions of all compounds were prepared in *DMSO. KCl* was used as electrolyte. Measurements were done by using three electrode assemblies in which a glassy carbon was used as working electrode, reference electrode was saturated calomel and a platinum wire was used as counter electrode. Firstly, experiment was performed with compound without DNA and second experiment was performed after the first DNA addition at varying scan rate of 100 mVs^{-1} to 700 mVs^{-1}. After this, a change in peak current and potential was observed by keeping the compound concentration constant and varying the concentration of DNA at a regular interval of time. Working electrode was cleaned after each reading. Binding constant on the account of decrease in peak current was calculated through the following equation 2 [27].

$$\frac{\log 1}{[DNA]} = \log K + \frac{\log I}{Io - I} \quad (2)$$

Binding site sizes were calculated by using the equation 3 [28].

$$\frac{Cb}{Cf} = \frac{K[free\ base\ pairs]}{s} \quad (3)$$

Results and Discussion

Spectroscopic Analysis

In the FT-IR spectrum of **FTU**, the presence of one band for NH at 3100 cm^{-1}, for C=O at 1681 cm^{-1}, *Fe-Cp* stretching at 483 cm^{-1} and the absence of strong band corresponds to isothiocyanate (N=C=S) around 2000 cm^{-1}, confirmed the successful formation of the ferrocenyl thiourea. In case of guanidine derivatives, the appearances of two NH bands between the ranges 3085-3232 cm^{-1}, and a characteristic band for CN_3 unit around 1528-1598 cm^{-1}, evident the guanidine formation. In the ^{1}H NMR spectrum of **FTU**, the presence of two NH signals at 12.6 and 11.5 ppm has given the confirmation of the thiourea formation. The aromatic protons gave

signals in the range of 7.60-8.01 ppm. A high intensity singlet at 4.05 ppm appeared due to five protons of unsubstituted cyclopentadienyl (*Cp*), whereas a signal corresponding to substituted *Cp* protons splits into two signals at 4.37 and 4.82 ppm. Due to the shifting of electron density of methyl towards the phenyl group, its signals appeared downfield at 3.3 ppm. In ^{1}H NMR spectra of guanidine derivatives, the shifting of signal from 12.6 to 10.8 ppm has given the clear indication that sulfur has been successfully replaced and appearance of signals in the range of 0.8-2.9 ppm confirmed that the alkyl chain has been attached. Methyl protons present at the end of aliphatic chain appeared around 0.8 ppm whereas the methylene protons near C=N are more desheilded and appeared in the range of 1.60-1.62 ppm.

In the ^{13}C-NMR spectrum of **FTU**, characteristic signals for C=S and C=O were present at 178 ppm and 168 ppm respectively, whereas four signals for *Fc-Cp* were also displayed in the region of 69.8 to 84.8 ppm. The unsubstituted *Cp* carbons gave a high intensity signal at 69.8 ppm whereas the substituted *Cp* carbons gave three signals, in which carbons directly attached to aromatic ring yielded a signal at 84.8 ppm and other four carbon exhibited signals around 66-69.4 ppm. Signals in the range of 124-137 ppm are due to the aromatic ring carbons. ^{13}C-NMR spectrum of the guanidine derivatives showed a characteristic signal for CN_3 unit at 151-152 ppm that confirmed the successful guanidine formation. By comparing with the ^{13}C spectrum of **FTU**, the disappearance of a signal around 178 ppm also evident that sulfur has been removed. All the aromatic and the ferrocenyl carbons are displayed in their typical range. Carbons of the long aliphatic chain appeared in the range of 14-31 ppm, having most deshielded methylene carbons at 28-31 ppm and a methyl carbon attached at terminal position appeared at 14 ppm.

Determination of Critical Micelles Concentration (CMC)

By Surface Tension Method

Among the various methods used for the *CMC* determination, tensiometry is a simple and principle method. Critical micelles concentrations for all the guanidine derivatives were measured through an automatic tensiometer and a decreasing trend of the surface tension was observed with the increasing surfactants concentration. Fig. 1 shows a plot of concentration (mM) of the guanidine surfactants *vs.* surface tension (mN/m) for **R-12G** in ethanol (22 mN/m at 25 ^{o}C). In the start of experiment, when the solvent has lower concentration of the surfactant, the surfactant molecules adsorbed at the air/solvent interface. Hence, a

continuous and constant lowering of surface tension was observed. After a certain point, the air/solvent interface is saturated and molecules start entering into the bulk solution and self-assemble, as a result a very minute decrease in surface tension was measured for the constant addition of surfactant. A plot between the surface tension *vs.* concentration gave two linear lines of different slopes as shown in Fig. 1 in which the breaking point gives the critical micelles concentration (*CMC*) as 00022 mM [29].
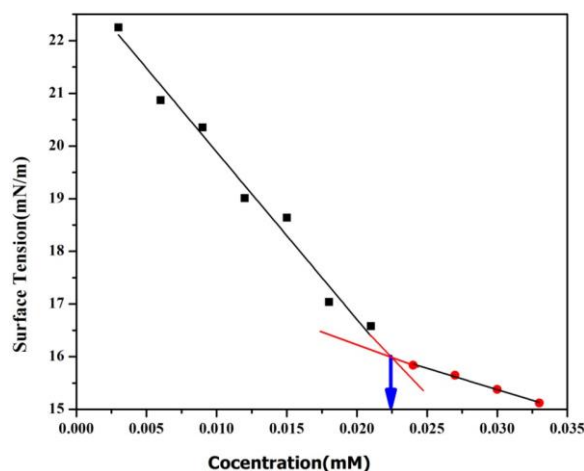

Fig. 1:   Plot for the determination of *CMC* by tensiometry (**RG-12**).

UV-Visible Method

UV-Visible method is an indirect method to determine the critical micelles concentration. The principle lies here is that the aggregates or micelles assemblies cause a hindrance in the passage of UV-Visible radiation through them. In the presence of lower concentrations of surfactant molecules in the solvent, there is a free passage for UV-Visible radiations to pass through and a linear relation exist between the concentrations *vs.* absorbance (Lambert Beer law). At higher surfactant concentrations, the molecules start self-aggregation and this linear relation deviates. When the concentration *vs.* absorbance graph is plotted it gives an inflection point by extra-plotting the two lines of different slopes. This inflection point helps to obtain the CMC point. By following this procedure UV-Visible spectrum of the synthesized surfactant was obtained as shown in the Fig. 2a and a plot of concentration (mM) *vs.* absorbance was plotted. The CMC values obtained by this method are listed in Table-1. Micellization usually does not occur at fixed concentration but in a certain concentration range. Hence, in case of **R-7G**, a smaller difference between the CMC values is noticed.
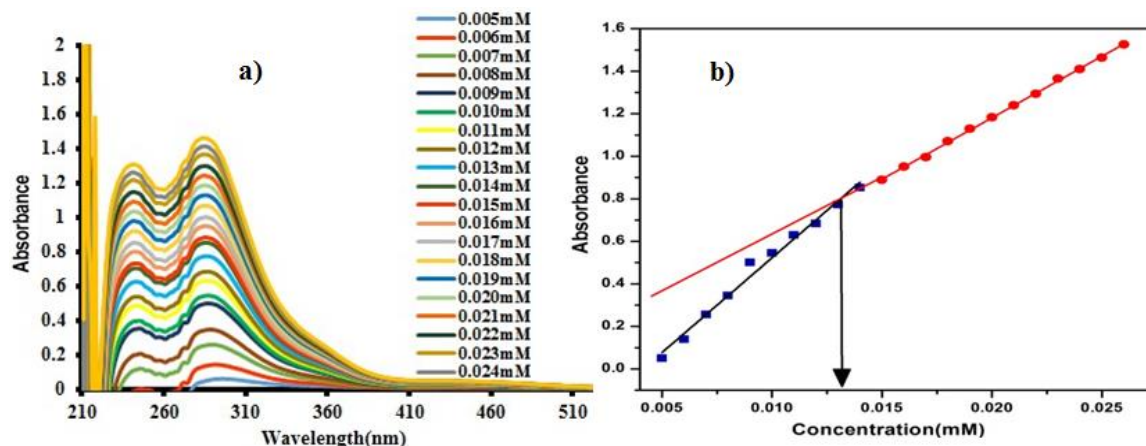
Fig. 2: a) UV-vis spectrum for different concentration of *RG-18* in ethanol, b) straight line graph for the determination of CMC of *RG-18*.

Comparison of CMC Values

CMC values obtained through the both methods are comparable with each other as shown in Table-1. CMC points for the ferrocenyl guanidine surfactants were calculated through the tensiometry and were further confirmed through UV-Visible spectroscopy. It was observed that *CMC* decreases with the increase in the alkyl chain length [29].

R18G< R-16G< R-12G < R-7G
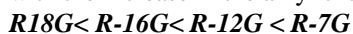
R-7G has a smaller chain length of seven carbon that show highest *CMC* whereas **R-18G** with a longest alkyl chain C18, has the lowest *CMC* value as determined through the both methods. All the synthesized surfactants have lower *CMC* in the range of 0.013 mM-0.049 mM. Nonionic surfactants usually have the lower *CMC* values than the ionic surfactants. Low values of *CMC* are due to the greater lipophilicity. Synthesized ferrocenyl surfactants have more lipophilic portion in their structure which facilitates the micellization at a low concentration [29].

Table-1: Comparison of CMC.

Compounds	CMC (mM) by surface tension method	CMC (mM) by UV-Visible spectroscopy
R-7G	0.039	0.049
R-12G	0.022	0.022
R-16G	0.019	0.019
R-18G	0.014	0.014

Computational Study

With the aims to optimize the molecular geometries and to evaluate quantum chemical parameters, density functional method (B3LYP/ 6-31G (d, p) in the gaseous phase) was employed. Fig 3a is showing the charge densities on each atom of

ferrocenyl thiourea through the color distribution. Charge densities were calculated *via* mulliken charges distribution. Darker to lighter colors scheme indicates the negative to positive charge distribution. As per color of carbon atoms of the phenyl and *Cp* rings, they have higher charge densities. A carbon atom of the phenyl ring that is directly attached to a methyl group has a higher charge density due to shifting of an electronic cloud from electron donating methyl group to that phenyl carbon atom. Nitrogen atoms also have negative charge densities. *Fe* atom is sandwiched between the two *Cp* rings and carbonyl attached to phenyl has a positive charge density. In the Fig. 3b it is noticed that in case of ferrocenyl guanidines, the carbon atom of CN_3 unit has a low charge density as it is attached to three electronegative nitrogen atoms. Color of a long carbon chain showing that the charge densities are comparable to *Cp* ring as it is a major lipophilic part of a surfactant. Hence, mulliken charges distribution also endorsed the assignment of lipophilic and lipophobic parts of guanidine based amphiphiles.

The frontier molecular orbitals (*HOMO* and *LUMO*) aid to locate the redox centers of the compounds [30]. Fig. 4 presents the molecular orbitals of the synthesized compounds. Band gaps (ΔE) calculated through UV-Visible spectroscopy were equally endorsed by the *DFT* calculations as listed in Table-3. A smaller difference in band gaps is observed *via* both method. Since the DFT calculations were performed in gaseous state, a smaller difference in band gaps is observed. Ferrocene owing redox active center, has a tendency to oxidize from +2 to +3 oxidation state. In case of *FTU*, the *HOMO* orbitals spread over the ferrocene and also extended towards the phenyl ring attached to

the ferrocene. Here, the delocalization of electronic cloud makes the oxidation process difficult. However, moving from *HOMO* to *LUMO* orbitals, the electronic cloud shift towards the benzoyl moiety.
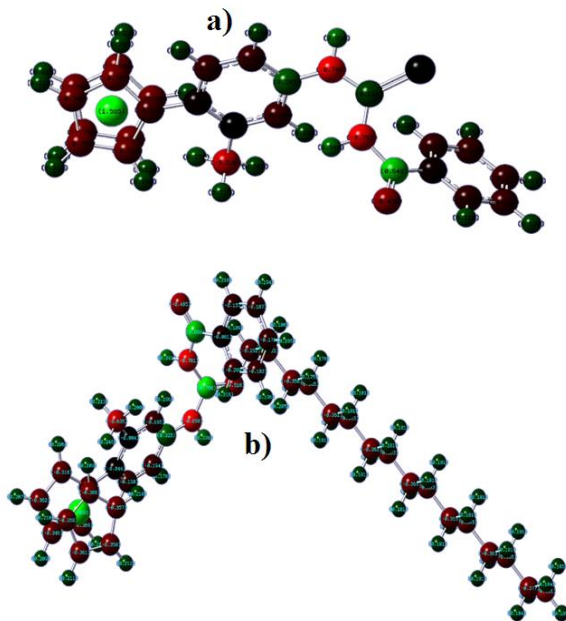

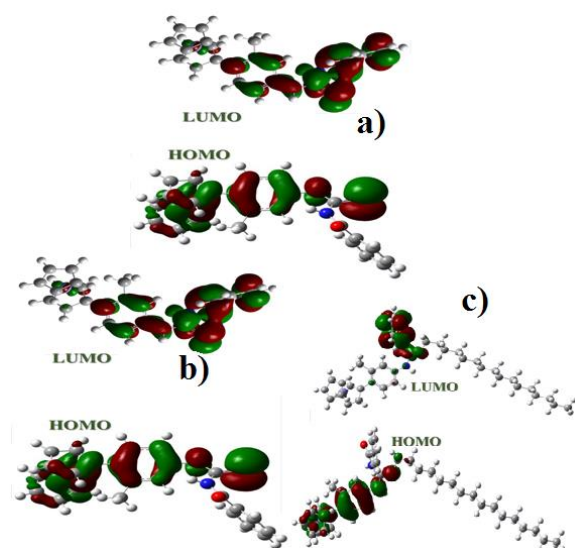Fig. 3: Mulliken charges distribution a) *FTU* b) *R16-G*.

Fig. 4: Representation of frontier orbitals and their associated band gaps a) *FTU* b) *RG-12*, c) *RG-16*.

In case of ferrocenyl guanidines, an electronic cloud is spread over symmetrical CN_3 unit, which makes the oxidation more facile and the E_{HOMO} decreases as compared to *FTU*. E_{HOMO} of *R-12G* is

5.19 eV and that of *FTU* is 5.58 eV. Due to which band gaps between the E_{HOMO} and E_{LUMO} increased. It was further confirm through UV-Visible spectroscopy. Reactivity and stability can easily be assessed through the band gap estimation. The slightly higher band gap of *R-18G* reflected its higher stability. This stability is associated with higher DNA binding constants as observed in DNA binding studies [31].

DNA Binding Studies

UV-Visible Spectroscopic Method

By employing this method, the drug/DNA interactions can be studied by measuring the absorbance with the increment of the DNA concentrations. The characteristic UV-Visible spectra of synthesized compounds have an intense peak in the UV range of 260-300 nm due to n→σ* electronic transitions. By keeping the drug concentration constant and adding a constant aliquant of DNA to the drug solution after regular time intervals, an increase in the absorbance was observed. This hyperchromic shift is indicating the electrostatic mode of binding and is attributed to the binding of Fc^{+3} ions of ferrocene with the phosphates of DNA [32-33]. As a result of these interactions, a double helical structure of DNA is disturbed since the interacting forces which hold the two strands together are weakened. DNA uncoiled into single strand and due to the presence of free bases in the solution, the absorbance of solution increased [34]. Spectra of *R-16G* (a) and *FTU* (c) in the Fig. 5 are showing an increasing trend of absorbance with the addition of DNA to the drug solutions of constant concentration and volume. Straight line graphs Fig. 5 (b and d) of *Ao/A-Ao vs.* 1/[DNA] are obtained by plotting the data from the spectra (a and c) for calculating binding constant (K_b) using the Benesi Hildebrand equation 2.

Binding constants for the synthesized thiourea and guanidine derivatives calculated by this method are listed in Table-3. Data revealed that the binding constant of a ferrocenyl thiourea *FTU* is lower than ferrocenyl guanidines. That indicates the superior potency of a guanidine moiety to interact with the living molecules. It is also noticed that the binding constant values of the synthesized guanidine surfactants increase by increasing the alkyl chain lengths. Moving from *R-7G* to *R-18G*, *R-18G* has a highest binding constant value and *R-7G* has a lowest. This can easily be explain by taking into account the lipophilic character. A molecules with the higher lipophilic character may show better interaction with the lipophilic center of DNA.
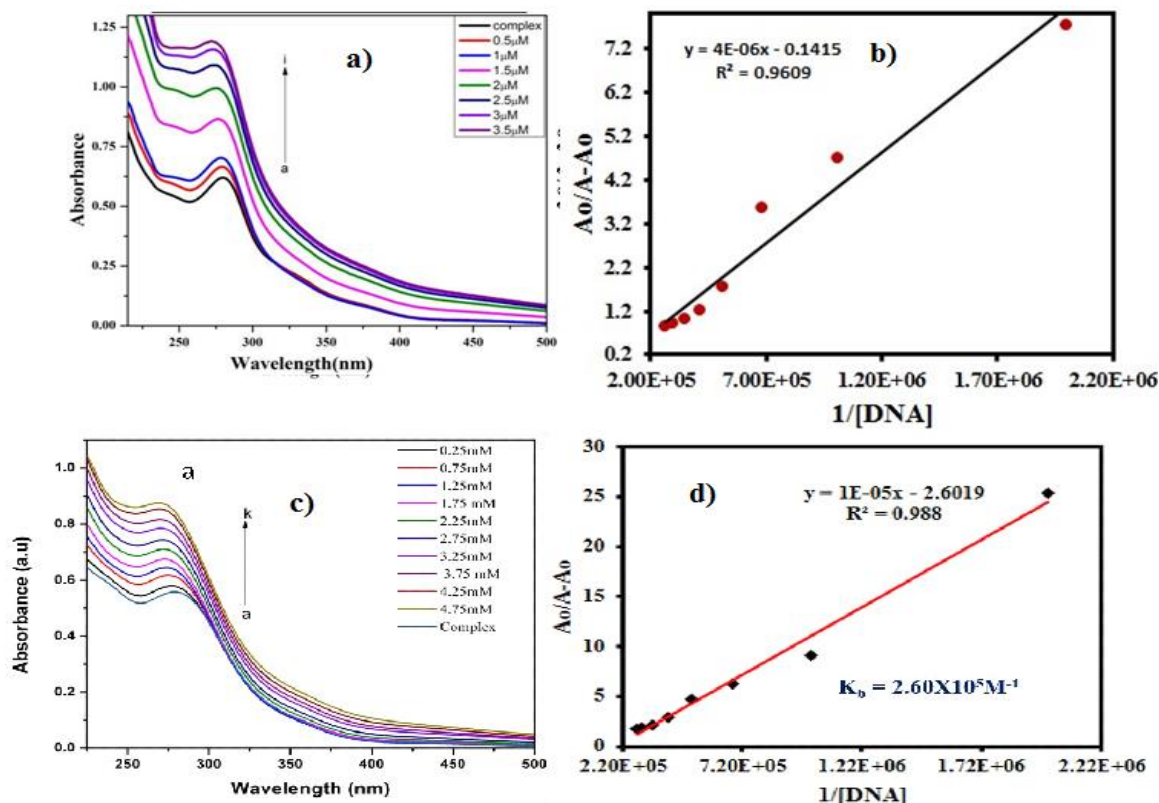
Fig. 5: a) UV-vis spectrum for *FTU*, (b) plots for determination of binding constant of *FTU*, (c) UV-Visible spectrum of *R-16G*, (d) binding constant plot for *R-16G*.

Table-3: Quantum chemical parameters for ferrocene-based thiourea and guanidine surfactants in gas phase at B3LYP/6-31G (d,p).

| Compounds | E_{HOMO} | E_{LUMO} | Band gap (ΔE) through DFT | Band gap (ΔE) through UV-visible spectroscopy |
	(eV)	(eV)	(eV)	(eV)
FTU	-5.58	-1.70	3.882	4.22
R7-G	-5.16	-1.21	3.950	4.23
R12-G	-5.19	-1.24	3.951	4.25
R16-G	-5.21	-1.26	3.954	4.27
R18-G	-5.22	-1.27-	3.955	4.28

Cyclic Voltammetric Method

Drugs / DNA interactions were also studied through a voltammatric method by employing an three electrodes assembly in *DMSO* at the scan rate of 100 mV/s. Experiments were run for the blank solutions of 1 mM synthesized compounds in a potential window of 0 to +1.3V at the varying scan rate of 100 mV/s to 700 mV/s. Subsequently, same experiment was repeated with a first DNA addition to the drug solutions of constant volume and concentration. Two voltammograms obtained by these experiments are shown in the Fig. 6 (a-b). Graphs between I (µA) and (V/s) $^{1/2}$ were plotted to find the diffusion coefficients of free drug and DNA bound drugs. Diffusion coefficient of a DNA bound drug is smaller than a free drug as shown in the Fig. 6c. This substantial decrease in the diffusion coefficient is attributed to the formation of the drug-DNA complex [35].

By constant addition of DNA to the drug solutions after regular intervals of time, a continuous decay in the peak current was noticed that is attributed to the stronger drug-DNA interaction. A positive shift of peak potential was also observed that is evident of the electrostatic mode of binding and is more likely due to the interaction of the Fc^{+3} ions with the negatively charged phosphate groups of DNA [36]. A graph between the log (1/DNA) and log I/Io-I is potted to calculate the binding constants (Fig. 7b). The binding sites are determined by plotting *Cb/Cf vs.* DNA concentration as presented in the Fig. 7(b). Interestingly, by continuously increasing the DNA concentration, a negative shift in peak current along with a small positive shift in the peak potentials is noticed as shown in the Fig. 7 (a) that signifying the intercalative mode of binding [37].
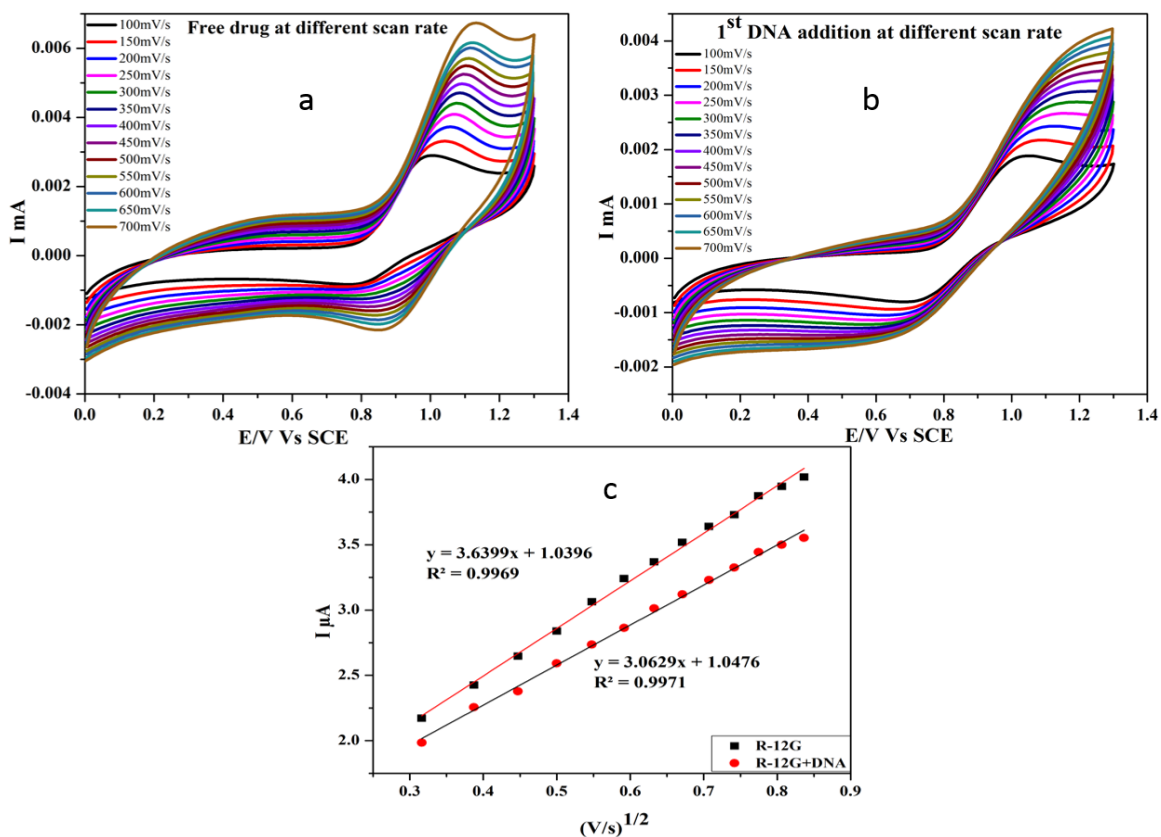
Fig. 6:   a) Voltammogram of **R-12G** from 100 to 700 mV/s, (b) Voltammogram of *R-12G*+ DNA from 100 to 700 mV/s, (c) plot for determination of diffusion coefficient.
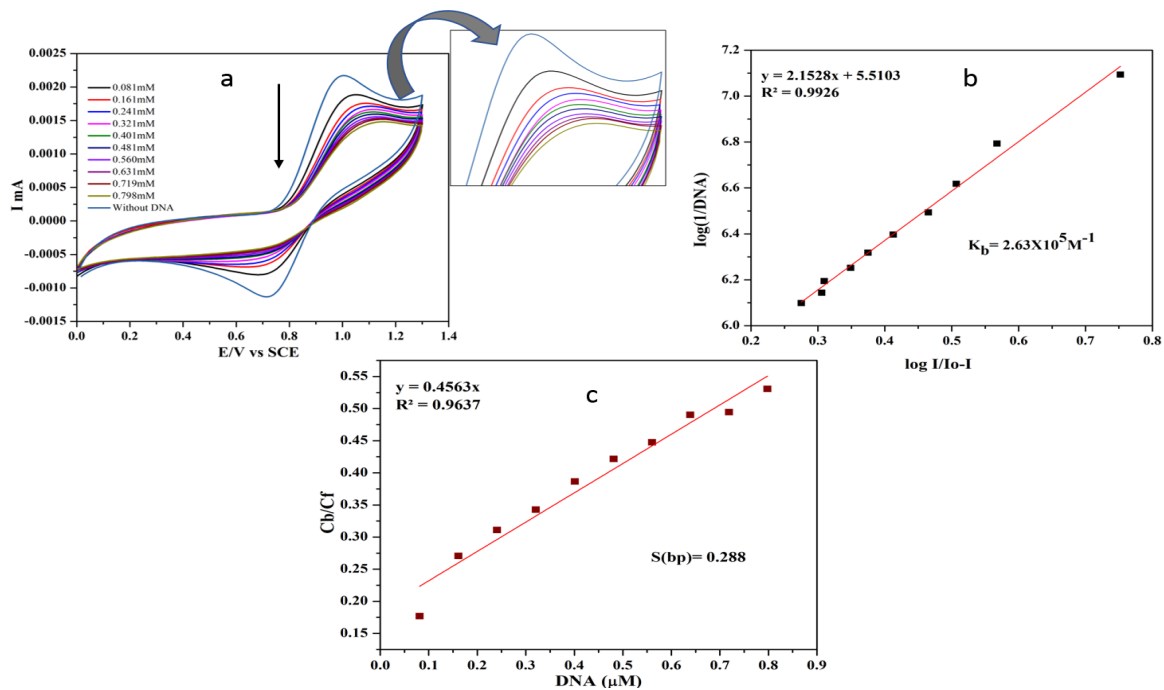

Fig. 7:   a) Voltammogram of **R-12G** at 100mV/s with different DNA concentrations, (b) plot for the determination of binding constant, (c) linear graph for calculating binding site size.

Table-3: Different parameters calculated from DNA-binding studies (UV, CV).

Compounds	Diff. coefficient (cm²/s)		K_b (CV)	S	K_b (UV)	ΔG
	Free Drug	Drug+DNA	M⁻¹	(bp)	M⁻¹	KJ/mol
R-18G	9.56×10^{-8}	8.51×10^{-8}	1.57×10^{6}	0.89	1.83×10^{5}	-30.02
R-16G	2.13×10^{-7}	1.33×10^{-7}	5.49×10^{5}	0.47	2.60×10^{5}	-30.89
R-12G	5.74×10^{-8}	5.23×10^{-8}	2.63×10^{5}	0.29	1.36×10^{5}	-29.29
R-7G	5.14×10^{-7}	4.91×10^{-7}	3.33×10^{5}	0.44	6.22×10^{4}	-27.35
FTU	2.37×10^{-7}	2.14×10^{-7}	6.02×10^{3}	0.10	3.54×10^{4}	-25.95

Binding constants obtained from the two techniques are comparable with each other and listed in the Table-3. It is concluded that the ferrocenyl thiourea (**FTU**) shows moderate electrostatic interaction with the binding constant value ~10^4 M⁻¹. Ferrocene based guanidine surfactants have higher binding constants in the range of 10^5 to 10^6 M⁻¹ that is clearly much higher than the thiourea. This is evident that the conversion of thiourea to CN_3 symmetrical functionality much increases the binding strength with DNA. Gibb's free energy is negative for this reaction which indicates the spontaneity of reaction and signifies that no external force is required to drive this drug-DNA interaction. Binding constants also show a linear depende nce on the lipophilicity of guanidine derivative as also determined by M.K. Amir *et al* [38]. In case of **RG-18** and **RG-16**, binding constants values calculated deviate from the normal trend (decreasing). This may be due to smaller difference of lipophilicity. Otherwise,binding constant values of rest of synthesized compound increased by increasing the hydrophobicity.

Conclusions

A ferrocene modified thiourea and four guanidines were synthesized and characterized by the spectroscopic methods. Lower critical micelles concentration points reveal that the incorporation of alkyl chain length can endowed surface activity and molecular aggregation properties. The results also imply that the surface activity is direct function of alkyl chain length. High DNA binding constants of ferrocene incorporated alkylguanides as compared to thiourea and phenylgunidines validated their superior DNA binding potentiality. This research study may provide an overlook to elaborate DNA interactions, a probable mechanism for designing new anti-cancer agents.

Conflicts of interest

There are no conflicts of interest to declare.

References

1. S. Patai, Chemistry of amidines and imidates. *Wiley:* (1975).

2. R. Gul, A. Khan, A. Badshah, M. K Rauf, A. Shah, Z. Rehman, A. Bano, R. Naz, M. N. Tahir, New Supramolecular Ferrocenyl Phenylguanidines as Potent Antimicrobial and DNA-Binding Agents, *J. Coord. Chem.,* **66,** 1959 (2013).

3. M. L. Williams, J. E. Gready, Guanidinium-Type resonance stabilization and its biological implications. I. the guanidine and extended-guanidine series, *J. Comput. Chem.,* **10,** 35(1989).

4. R. D. Kenyes, Ion channels in the nerve-cell membrane, *Sci. Am.* **240,** 126 (1979).

5. H. Zhang, C. Crogran-Grundy, C. May, J. Drewe, B. Tseng, S. X. Cai, Discovery and structure–activity relationships of (2-(arylthio) benzylideneamino) guanidines as a novel series of potent apoptosis inducers, *Bioorg. Med. Chem.*, **7,** 2852 (2009).

6. K. Umezawa, T. Takeuchi, Spergualin: a new antitumour antibiotic, *Biomed. Pharmacother*., **41,** 227 (1987).

7. K. Brozewicz, J. Stawinski, 1-(2-Mercaptobenzenesulfonyl)-3-hydroxyguanidines–Novel potent antiproliferatives, synthesis and in vitro biological activity, *Eur. J. Med. Chem*., **55,** 384 (2012).

8. B. Lal, A Badshah, A. A. Altaf, M. N. Tahir, S. Ullah, F. Huq, Study of new ferrocene incorporated N, N' disubstituted thioureas as potential antitumour agents, *Aust. J. Chem.,* **66.** 1352 (2013).

9. E. Bingham, B. Cohrssen, C. H. Powell, *Patty'stoxicology John Wiley & Sons. New York,* p. V2 43 (2001)

10. S. Top, A. Vessières, G. Leclercq, J. Quivy, J. Tang, J. Vaissermann, M. Huché, G. Jaouen, Synthesis, biochemical properties and molecular modelling studies of organometallic specific estrogen receptor modulators (SERMs), the ferrocifens and hydroxyferrocifens: evidence for an antiproliferative effect of hydroxyferrocifens on both hormone-dependent and hormone-independent breast cancer cell lines, *Eur. J. Chem.,* **9,** 5223 (2003).

11. C. Biot, N. Chavain, F. Dubar, B. Pradines, X. Trivelli, J. Brocard, I. Forfar, D. Dive, Structure–

activity relationships of 4-N-substituted ferroquine analogues: Time to re-evaluate the mechanism of action of ferroquine. *J. Organomet. Chem.,* **694**, 845 (2009) 845-854.

12. M. F. Fouda, M. M. Abd-Elzaher, R. A. Abdelsamaia, A. A. Labib, On the medicinal chemistry of ferrocene, *Appl. Organomet. Chem.*, **21**, 613 (2007).

13. A. Chesney, M. R. Bryce, R. W. Chubb, A.S. Batsanov, J. A. Howard, Chiral ferrocenyl-oxazolines incorporating thioether units: effective ligands for palladium-catalysed allylic substitution, *Tetrahedron: Asymm.,* **8,** 2337 (1997).

14. H. Tsukube, H. Fukui, S. Shinoda, Synergistic binding and chirality sensing of unprotected amino acids with ferrocenecarboxylic acid–crown ether conjugate, *Tetrahedron Lett.,* **42**, 7583 (2001).

15. R. Kumar, S. R. Dhakate, P. Saini, R.B. Mathur, Improved electromagnetic interference shielding effectiveness of light weight carbon foam by ferrocene accumulation, RSC *Advances,* **3**, 4145 (2013).

16. H. Wei, C. Y. Quan, C. Chang, X. Z. Zhang, R. X. Zhuo, Preparation of novel ferrocene-based shell cross-linked thermoresponsive hybrid micelles with antitumor efficiency, *,J. Phys. Chem. B,* **114**, 5309 (2010).

17. H. Kuwahara, M. Hamada, Y. Ishikawa, T. Kunitake, Self-organization of bilayer assemblies in a fluorocarbon medium, *J. Am. Chem. Soc.*, **115,** 3002 (1993).

18. Y. Ishikawa, H. Kuwahara, T. Kunitake, Self-assembly of bilayers from double-chain fluorocarbon amphiphiles in aprotic organic solvents: thermodynamic origin and generalization of the bilayer assembly, *J. Am. Chem. Soc.*, **116**, 5579 (1994).

19. S. Fatima, A. Badshah, B. Lal, F. Asghar,M. N. Tahir, A. Shah, I. Ullah, Study of new ferrocene-based thioureas as potential nonionic surfactants, *J. Organomet. Chem.*, **819**, 194 (2016).

20. F. Asghar, S. Fatima, S. Rana, A. Badshah, I. S. Butler, M. N. Tahir, Synthesis, Spectroscopic Investigation, and DFT Study of: N, N ′-Disubstituted Ferrocene-Based Thiourea Complexes as Potent Anticancer Agents, *Dalt. Trans.*, **47,** 1868 (2018).

21. F. Asghar, F.; Badshah, A.; I. S. Butler, S. Tabassum, B. Lal, M. N. Tahir, Bioactivity of new ferrocene incorporated N,N0-disubstituted ureas: Synthesis, structural elucidation and DFT study, *Inorganica Chim. Acta.,* **442**, 46 (2016).

22. R. Gul, A. Khan, A. Badshah, M. K. Rauf, A. Shah, Z. Rehman, M. N. T New Supramolecular Ferrocenyl Phenylguanidines as Potent Antimicrobial and DNA-Binding ahir, *J. Coord. Chem.,* **66**, 1959 (2013).

23. R. Gul, R.; M. K. Rauf, A. Badshah,S. Sikander, M. Nawaz,A. Khan Ferrocene-Based Guanidine Derivatives : In Vitro Antimicrobial, DNA Binding and Docking Supported Urease Inhibition Studies,, *Eur. J. Med. Chem.,* **85**, 438 (2014).

24. R. Gul Synthesis and Biological Evaluation of Some New Ferrocenyl Phenyl Guanidines as Antibacterial, Antifungal Agents,, *J. Drug Des. Med. Chem.,* **2**, 35 (2016).

25. S. Ali, A. Badshah, H. Hussain, S. Fatima, A. Hassan and S. Afzal. Synthesis, Characterization, and Computational Study of New Ferrocene-Based Schiff Bases as Potential Nonionic Surfactants, (2019). doi:10.1002/jsde.12282.

26. S. Zubair, F. Asghar, A. Badshah, B. Lal, R. A. Hussain, S. Tabassum, M. N. Tahir, New Bioactive Ferrocene-Substituted Heteroleptic Copper(I) Complex: Synthesis, Structural Elucidation, DNA Interaction, and DFT Study, *J. Organomet. Chem.,* **879**, 60 (2019).

27. N. Khan, B. Lal, A. Badshah, A.A. Altaf, S. Ali, S. Kamal, Zia-ur-Rehman "DNA binding studies of new Ferrocene based Bimetallics J. Chem. Soc. Pak., **35**, 916 (2013).

28. F. Asghar,, S. Rana, S. Fatima, A. Badshah, B. Lal, I.S. Butler, Biologically active halo-substituted ferrocenyl thioureas: synthesis, spectroscopic characterization, and DFT calculations, *New J. Chem.,* **42**, 7154 (2018).

29. S. Fatima, R. Sharma, F. Asghar, A. Kamal, A. Badshah, H. B Kraatz, Study of New Amphiphiles Based on Ferrocene Containing Thioureas as Efficient Corrosion Inhibitors: Gravimetric, Electrochemical, SEM and DFT Studies. Journal of Industrial and Engineering Chemistry, *J. Ind. Eng. Chem.,* **76**, 347 (2019).

30. F. Asghar, A. Badshah, B. Lal, S. Zubair, S. Fatima, I.S. Butler, Facile synthesis of fluoro, methoxy, and methyl substituted ferrocene-based urea complexes as potential therapeutic agents, *Bioorg. Chem.*, **72**, 215 (2017).

31. S. Zeb, M. Kashif, I. Ullah, A. Aamir, J. M. Pezzuto, T. Kondratyuk, F. Bélanger-gariepy, A. Ali, S. Khan, Zia-ur-Rehman, New heteroleptic palladium(II) dithiocarbamates: synthesis, characterization, packing and anticancer activity

against five different cancer cell lines, *Appl. Organomet. Chem.*, **30**, 392 (2016).

32. M. Imran, Zia-ur-Rehman, T. Kondratyuk, F. Bélanger-gariepy, New ternary platinum(II) dithiocarbamates: Synthesis, characterization, anticancer, DNA binding and DNA denaturing studies, *Inorg. Chem. Commun.*, **103**, 12 (2019).

33. Zia-ur-Rehman, A. Shah, M. N. Muhammad, S. Ali, R. Qureshi, A. Meetsma, I. Sydney, Synthesis, spectroscopic characterization, X-ray structure and evaluation of binding parameters of new triorganotin(IV) dithiocarboxylates with DNA, *Eur. J. Med. Chem.,* **44**, 3986 (2009).

34. M. Kashif, Zia-ur-Rehman, F. Hayat, S. Z. Khan, G. Hogarth, T. Kondratyuk, M. J. Pezzuto, M. N. Tahir, Monofunctional platinum(II) dithiocarbamate complexes: Synthesis, characterization and anticancer activity, *RSC Adv.,* **6**, 110517 (2016).

35. S. Hussain, A. Badshah, B. Lal, R. A. Hussain, S. Ali, M. N. Tahir, A. A. Altaf,, New supramolecular ferrocene incorporated N, N′-disubstituted thioureas: synthesis, characterization, DNA binding, and antioxidant studies, *J. Coord. Chem.*, **67**, (2014) 2148-2159.

36. R. A. Hussain, A. Badshash, M. Sohail, B. Lal, A. A. Altaf, Synthesis, chemical

37. characterization, DNA interaction and antioxidant studies of ortho, meta and para fluoro substituted ferrocene incorporated selenoureas selenoureas, *Inorganica Chim. Acta.,* **402**, 133 (2013).

38. B. Lal, A. Badshah, A. A. Altaf, M. N. Tahir, I. Ullah, F. Huq, Synthesis, Characterization and Antitumor activity of new Ferrocene incorporated N, N disubstituted Thioureas *Dalt. Trans.,* **41**, 14643 (2012).

39. M. Kashif, S. Zeb, F. Hayat, A. Hassan, I. S. Butler, Zia-ur-Rehman, Anticancer activity, DNA-binding and DNA-denaturing aptitude of palladium(II) dithiocarbamates, *Inorganica Chim. Acta.*, **451**, 31 (2016).